

# Passive mode-locking of a diode-pumped Nd:YVO<sub>4</sub> laser by intracavity SHG in PPKTP

Hristo Iliev<sup>1</sup>, Danail Chuchumishev<sup>1</sup>, Ivan Buchvarov<sup>1\*</sup>, and Valentin Petrov<sup>2</sup>

<sup>1</sup>Department of Quantum Electronics, Faculty of Physics, Sofia University, 5 James Bourchier Blvd., BG-1164 Sofia, Bulgaria,

<sup>2</sup>Max-Born-Institute for Nonlinear Optics and Ultrafast Spectroscopy, 2A Max-Born-Str. D-12489 Berlin, Germany  
[\\*ibuch@phys.uni-sofia.bg](mailto:*ibuch@phys.uni-sofia.bg)

**Abstract:** Experimental results on passive mode-locking of a Nd:YVO<sub>4</sub> laser using intracavity frequency doubling in periodically poled KTP (PPKTP) crystal are reported. Both, negative cascaded  $\chi^{(2)}$  lensing and frequency doubling nonlinear mirror (FDNLM) are exploited for the laser mode-locking. The FDNLM based on intensity dependent reflection in the laser cavity ensures self-starting and self-sustaining mode-locking while the cascaded  $\chi^{(2)}$  lens process contributes to substantial pulse shortening. This hybrid technique enables generation of stable trains of pulses at high-average output power with several picoseconds pulse width. The pulse repetition rate of the laser is 117 MHz with average output power ranging from 0.5 to 3.1 W and pulse duration from 2.9 to 5.2 ps.

©2010 Optical Society of America

**OCIS codes:** (140.4050) Mode-locked lasers; (140.3530) Lasers, neodymium; (140.3480) Lasers, diode-pumped

---

## References and links

1. U. Keller, "Recent developments in compact ultrafast lasers," *Nature* **424**(6950), 831–838 (2003).
2. G. Cerullo, S. De Silvestri, A. Monguzzi, D. Segala, and V. Magni, "Self-starting mode locking of a cw Nd:YAG laser using cascaded second-order nonlinearities," *Opt. Lett.* **20**(7), 746–748 (1995).
3. A. Agnesi, A. Lucca, G. Reali, and A. Tomaselli, "All-solid-state high-repetition-rate optical source tunable in wavelength and in pulse duration," *J. Opt. Soc. Am. B* **18**(3), 286–290 (2001).
4. U. Keller, K. J. Weingarten, F. X. Kärtner, D. Kopf, B. Braun, I. D. Jung, R. Fluck, C. Hönninger, N. Matuschek, and J. Aus der Au, "Semiconductor saturable absorber mirrors (SESAM's) for femtosecond to nanosecond pulse generation in solid-state lasers," *IEEE J. Sel. Top. Quantum Electron.* **2**(3), 435–453 (1996).
5. J. Kleinbauer, R. Knappe, and R. Wallenstein, "Ultrashort pulse lasers and amplifiers based on Nd:YVO<sub>4</sub> and Yb:YAG bulk crystals," in *Femtosecond Technology for Technical and Medical Applications*, F. Dausinger, F. Lichtner, H. Lubatschowski (Eds.), Topics in Applied Physics, Vol. 96, Springer (Berlin, 2004), pp.17-33.
6. T. Graf, A. I. Ferguson, E. Bente, D. Burns, and M. D. Dawson, "Multi-Watt Nd:YVO<sub>4</sub> laser, mode locked by a semiconductor saturable absorber mirror and side-pumped by a diode-laser bar," *Opt. Commun.* **159**(1-3), 84–87 (1999).
7. D. Burns, M. Hetterich, A. I. Ferguson, E. Bente, M. D. Dawson, J. I. Davies, and S. W. Bland, "High-average-power (> 20-W) Nd:YVO<sub>4</sub> lasers mode locked by strain-compensated saturable Bragg reflectors," *J. Opt. Soc. Am. B* **17**(6), 919–926 (2000).
8. Y. F. Chen, S. W. Tsai, Y. P. Lan, S. C. Wang, and K. F. Huang, "Diode-end-pumped passively mode-locked high-power Nd:YVO<sub>4</sub> laser with a relaxed saturable Bragg reflector," *Opt. Lett.* **26**(4), 199–201 (2001).
9. G. J. Spühler, T. Südmeyer, R. Paschotta, M. Moser, K. J. Weingarten, and U. Keller, "Passively mode-locked high-power Nd:YAG lasers with multiple laser heads," *Appl. Phys. B* **71**, 19–25 (2000).
10. L. McDonagh, R. Wallenstein, and A. Nebel, "111 W, 110 MHz repetition-rate, passively mode-locked TEM<sub>00</sub> Nd:YVO<sub>4</sub> master oscillator power amplifier pumped at 888 nm," *Opt. Lett.* **32**(10), 1259–1261 (2007).
11. Y. F. Chen, S. W. Tsai, and S. C. Wang, "High-power diode-pumped nonlinear mirror mode-locked Nd:YVO<sub>4</sub> laser with periodically-poled KTP," *Appl. Phys. B* **72**, 395–397 (2001).
12. A. Agnesi, C. Pennacchio, G. C. Reali, and V. Kubecek, "High-power diode-pumped picosecond Nd<sup>(3+)</sup>:YVO<sub>4</sub> laser," *Opt. Lett.* **22**(21), 1645–1647 (1997).
13. I. C. Buchvarov, and S. M. Saltiel, "Passive feedback control of actively mode-locked pulsed Nd:YAG laser," *Proc. SPIE* **1842**, 124–129 (1992).
14. I. C. Buchvarov, K. A. Stankov, and S. M. Saltiel, "Pulse shortening in an actively mode-locked laser with a frequency-doubling nonlinear mirror," *Opt. Commun.* **83**(3-4), 241–245 (1991).
15. K. A. Stankov, and J. Jethwa, "J., "A new mode-locking technique using a nonlinear mirror," *Opt. Commun.* **66**(1), 41–46 (1988).

16. I. Buchvarov, G. Christov, and S. Saltiel, "Transient behavior of frequency doubling mode-locker. Numerical analysis," *Opt. Commun.* **107**(3-4), 281–286 (1994).
17. S. J. Holmgren, V. Pasiskevicius, and F. Laurell, "Generation of 2.8 ps pulses by mode-locking a Nd:GdVO<sub>4</sub> laser with defocusing cascaded Kerr lensing in periodically poled KTP," *Opt. Express* **13**(14), 5270–5278 (2005).
18. A. Agnesi, A. Guandalini, A. Tomaselli, E. Sani, A. Toncelli, and M. Tonelli, "Diode-pumped passively mode-locked and passively stabilized Nd<sup>3+</sup>:BaY<sub>2</sub>F<sub>8</sub> laser," *Opt. Lett.* **29**(14), 1638–1640 (2004).
19. P. K. Yang, and J. Y. Huang, "An inexpensive diode-pumped mode-locked Nd:YVO<sub>4</sub> laser for nonlinear optical microscopy," *Opt. Commun.* **173**(1-6), 315–321 (2000).
20. K. A. Stankov, "A mirror with an intensity-dependent reflection coefficient," *Appl. Phys. B* **45**(3), 191–195 (1988).
21. I. Ch. Buchvarov, P. N. Tzankov, V. Stoev, K. Demerdjiev, and D. Shumov, "Generation of high power picosecond pulses by passively mode-locked Nd:YAG laser using frequency doubling mirror," in *Advanced Photonics with Second-Order Optically Nonlinear Processes: 61* (NATO Science Series. Partnership Sub-Series 3, High Technology), A.D. Boardman, L. Pavlov, and S. Tanev (eds), Kluwer Academic Publishers, Dordrecht, Netherlands, (1998), pp. 197–200.
22. K. Kato, and E. Takaoka, "Sellmeier and thermo-optic dispersion formulas for KTP," *Appl. Opt.* **41**(24), 5040–5044 (2002).
23. G. D. Boyd, and D. A. Kleinman, "Parametric interaction of focused Gaussian light beams," *J. Appl. Phys.* **39**(8), 3597–3639 (1968).
24. E. Innerhofer, T. Südmeyer, F. Brunner, R. Häring, A. Aschwanden, R. Paschotta, C. Hönniger, M. Kumkar, and U. Keller, "60-W average power in 810-fs pulses from a thin-disk Yb:YAG laser," *Opt. Lett.* **28**(5), 367–369 (2003).

## 1. Introduction

Nowadays, diode-pumped mode-locked neodymium (Nd) lasers operating at ~100 MHz repetition rate, are the main source of high average power picosecond pulses with duration ranging from a few up to more than hundred picoseconds [1–4]. Such laser sources are particularly attractive for nonlinear optics and spectroscopy as well as for applications in medical diagnostics and micro-machining. In general, much shorter pulses can be generated with passive mode-locking which, in contrast to active mode-locking techniques, does not require external driving source and the repetition rate is determined solely by the round trip time of the cavity [1].

With few exceptions, e.g. the additive mode-locking [5], multi-Watt operation of picosecond diode-pumped Nd oscillators has been demonstrated mainly by two passive mode-locking methods, one based on semiconductor saturable absorber mirrors (SESAMs) [6–8] and the other - on intracavity frequency doubling. The highest average powers demonstrated so far with SESAM technology and Nd:YVO<sub>4</sub> or Nd:YAG are in excess of 20 W [7–9], reaching 56 W with pumping at 888 nm [10]. Although SESAMs are well established devices for lasers emitting around 1 μm, their residual absorption, leading to heating, is the major intrinsic drawback which determines their damage threshold (current state of the art is ~0.5 GW/cm<sup>2</sup> at 20 ps pulse duration) [7] and limits their power scaling capabilities. Intracavity frequency doubling is a promising mode-locking approach for up-scaling the power of such picosecond solid-state lasers because the damage threshold of nonlinear crystals is an order of magnitude higher and the low residual absorption at the fundamental wave enables operation at high average power. Furthermore, this approach is easily extendable to any laser spectral region.

In the case of intracavity type-I second-harmonic generation (SHG), two different passive mode-locking mechanisms can be utilized. The first one is based on the intensity dependent reflectivity of the frequency-doubling nonlinear mirror (FDNLM), consisting of a crystal for SHG, a dielectric mirror, and dispersive medium between them [11–14]. In this scheme, the second harmonic generated upon passing through the nonlinear crystal (NLC) is completely reflected by the dielectric mirror and interacts again with the fundamental on its way back through the same nonlinear crystal, thus a double-pass (cascaded) SHG process takes place. The dielectric mirror should be a dichroic mirror (DM), having comparatively low reflectivity at the fundamental and high reflectivity at the second harmonic. Hence, the reflectivity of the combination, crystal for SHG and a dielectric mirror, called FDNLM, is governed by the back conversion from second harmonic to the fundamental [13,15]. The dispersive medium determines the relative phase shift of the fundamental and second harmonic waves

accumulated between the NLC and the DM. The main drawback of the FDNLM is the longer duration of the output pulse in comparison with the pulse traveling inside the laser cavity [16]. The second mode-locking mechanism is based on cascaded  $\chi^{(2)}$  lens formation [2,17]. It does not exhibit the pulse duration limitation characteristic for the FDNLM. Thus, it provides shorter pulses but higher nonlinearity is required for self-starting mode-locking. Also, this technique is sensitive to external perturbations. In this respect, cascaded  $\chi^{(2)}$  lens mode-locking assisted by FDNLM has a potential which has not been exploited effectively, yet [18], although this is a natural combination of two effects taking place in the same mode-locking device, in contrast to combining cascaded  $\chi^{(2)}$  lens formation with a SESAM [19]. Moreover, the potential of quasi-phase-matched materials with their high effective nonlinearity and absence of spatial walk-off seems not to have been properly utilized. There are only a few reports in which SHG in periodically poled KTP (PPKTP) has been employed for passive mode-locking [11,17]. The highest average output power (5.6 W with Nd:YVO<sub>4</sub>) in the steady state regime was achieved in [11] using a FDNLM based on PPKTP but the pulse duration (20 ps) does not fully utilize the gain bandwidth of the active medium. Much shorter pulses of 2.8 ps were obtained in [17] with a Nd:GdVO<sub>4</sub> laser by cascaded  $\chi^{(2)}$  lens formation in PPKTP but at the expense of rather low (350 mW) average output power.

In this work we investigate passive mode-locking of a Nd:YVO<sub>4</sub> laser using intracavity SHG in PPKTP. The FDNLM initiates the passive mode-locking process and ensures self-sustained operation while the defocusing cascaded  $\chi^{(2)}$  effect leads to the shortest pulse duration of 2.9 ps. Thus, although each of the two mode-locking mechanisms in principle can be used alone for passive mode-locking of the laser, the hybrid scheme proves beneficial for the robust laser performance in this study. The output power is ranging from 0.5 to 3.1 W, close to the maximum value for TEM<sub>00</sub> CW operation of the laser.

## 2. Experimental set-up

The design of the mode-locked laser is based on a 1.4 m long linear cavity (Fig. 1). The active element (AE) is a 5-mm long, 0.5 at. % doped Nd:YVO<sub>4</sub> crystal with an aperture of 2.5 × 2.5 mm<sup>2</sup>. The *a*-cut sample is 1.5°-wedged. It is pumped by a 50-W 808-nm laser diode bar coupled into a 400 μm optical fiber (NA = 0.22). The AE is mounted in a metal holder maintained at a temperature of 25°C by running water. The resonator end mirrors are the high-reflective rear face of the AE and the flat output coupler (OC). The other face of the AE is antireflection coated. The radius of curvature of the folding mirror M1 and the focal length of the lens F3 (80 mm) are chosen to ensure beam radius of 80 μm in the nonlinear crystal and 200 μm in the AE. Single transverse mode operation is achieved by overlapping the resonator eigenmode with the pump waist formed by the objective lenses F1 and F2.

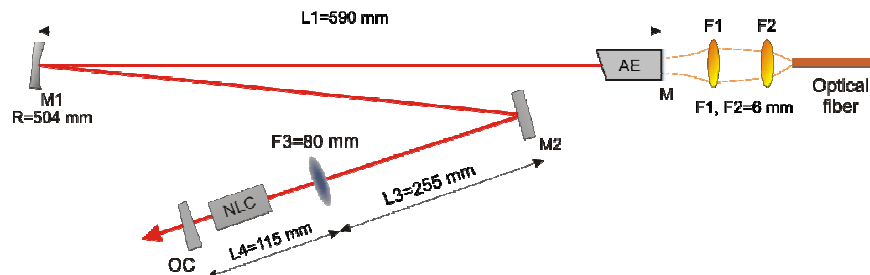


Fig. 1. Schematic of the laser cavity: F1, F2 – pump objective; AE - Nd:YVO<sub>4</sub> active element; M, M1, M2 - highly reflecting mirrors at the fundamental wavelength, F3 - focusing lens, NLC - PPKTP nonlinear crystal, OC - output coupler.

After initial cavity alignment, the distance between lens F3 and output coupler OC is optimized for maximum output power in the fundamental transverse mode - TEM<sub>00</sub>. The laser operates in  $\pi$ -polarization. The distance between the NLC and OC is set around 25 mm. This distance is optimized for each mode-locking experiment by translating the NLC in order to achieve self-starting and continuous mode-locked operation. The NLC is a 1-mm thick

PPKTP crystal with 8.94  $\mu\text{m}$  poling period, a length of 5 mm (along the x-axis) and a width of 5 mm (along the y-axis), antireflection coated for both the fundamental and the second harmonic. It is designed for SHG at 1064.2 nm at a temperature of 70°C. The PPKTP crystal is mounted in an oven with high precision (0.1°C) temperature control.

### 3. Mode-locking technique

The intracavity type-I SHG provides two different types of passive mode-locking mechanisms: The first one is amplitude shaping and based on the intensity dependent reflectivity of the FDNLM and the second one is phase shaping and based on cascaded  $\chi^{(2)}$  nonlinear phase shift of the fundamental wave, i.e. cascaded  $\chi^{(2)}$  lens mode-locking.

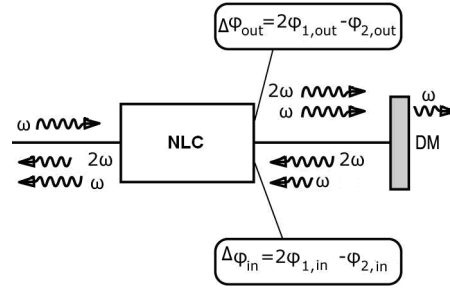


Fig. 2. Schematic of the FDNLM: NLC, nonlinear SHG crystal; DM, dichroic mirror.

A schematic of the FDNLM is shown on Fig. 2. The FDNLM consists of the frequency doubling NLC and the dichroic mirror DM, high reflecting at the second harmonic ( $2\omega$ ) and partially reflecting at the fundamental ( $\omega$ ) wavelength. In general, the reflection by the FDNLM includes a two-way pass of the beam through the NLC. At perfect phase-matching of the SHG, the FDNLM reflection is governed by the SHG conversion efficiency which is a function of the input beam intensity and the phase difference  $\Delta\varphi_{in} = 2\varphi_{1,in} - \varphi_{2,in}$  between the fundamental and second harmonic wave in the beginning of the second pass through the NLC. If  $\Delta\varphi_{in} = \Delta\varphi_{out} \pm (2m + 1)\pi$ ,  $m = 0, 1, 2, \dots$ , see Fig. 2, the second harmonic is partially reconverted into the fundamental on the way back, leading to increase of the FDNLM reflectivity at the fundamental wavelength. The higher the intracavity intensity, the higher will be the FDNLM reflectivity with respect to the fundamental wave. If the DM reflects partially the fundamental wave, the value of the FDNLM reflectivity can be higher than the value of the linear reflectivity of this mirror. Thus the FDNLM introduces a positive nonlinear feedback into the laser resonator. The nonlinear reflectivity  $R_{NL}$  normalized to the reflectivity  $R_{\omega}$  of the dichroic mirror is shown on Fig. 3a as a function of the single pass SHG efficiency. In the case of  $\Delta\varphi_{in} = \Delta\varphi_{out} \pm 2m\pi$ ,  $m = 0, 1, 2, \dots$ , in the second pass through the nonlinear crystal, the phase difference  $\Delta\varphi_{in}$  between the fundamental and the second harmonic waves enables further conversion of the fundamental into the second harmonic wave leading to further decrease of the fundamental beam intensity. Thus the FDNLM introduces a negative nonlinear feedback and the FDNLM reflectivity decreases with increasing intensity of the fundamental beam, i.e. with increasing single pass SHG efficiency, see Fig. 3b. The proper adjustment of the value of  $\Delta\varphi_{in}$  for specific FDNLM operation is realized by changing the distance between NLC and DM or by slightly rotating a glass plate placed between the NLC and DM. In both cases the dispersion in air and glass causes change in  $\Delta\varphi_{in}$ . Originally the FDNLM was proposed first by Stankov [20] as a mode-locking technique based on perfectly phase-matched SHG.

In the presence of phase-mismatch, the back conversion to the fundamental upon the second pass through the NLC depends on the phase shift  $\Phi = \Delta\phi_m + \Delta kL$ , where  $\Delta k = k_2 - 2k_1$  is the wave vector mismatch, and  $L$  is the length of the SHG crystal. Hence, the intensity dependent reflectivity of the FDNLM is a function of the additional parameter  $\Delta kL$  which leads to new requirements for  $\Delta\varphi_{in}$  in comparison to the perfect phase matching case.

Figure 4 shows the normalized nonlinear reflectivity  $R_{\text{NL}}/R_{\omega}$  of the FDNLM, the pulse shortening ratio  $\tau_{\text{out}}/\tau_{\text{in}}$ , equal to the reflected pulse duration  $\tau_{\text{out}}$  divided by the pulse duration of the input pulse  $\tau_{\text{in}}$ , and the nonlinear phase shift  $\varphi_1$  of the fundamental wave reflected by the FDNLM.

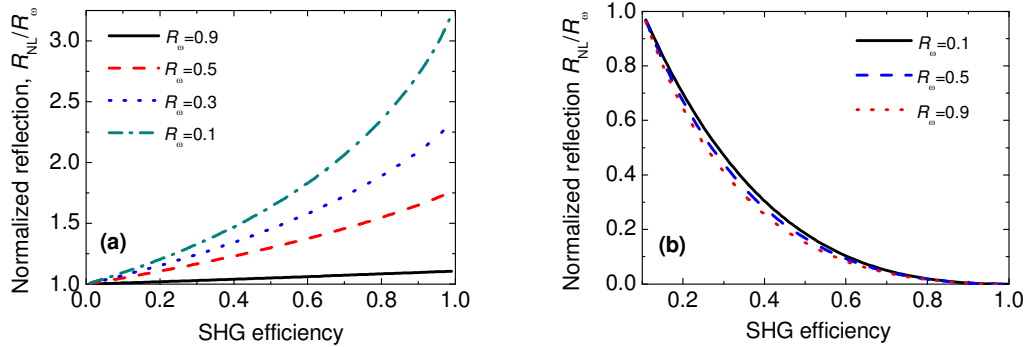


Fig. 3. Analytically calculated normalized FDNLM reflection as a function of the SHG efficiency for perfect phase matching and different  $R_{\omega}$ , (a)  $\Delta\varphi_{\text{in}} = \Delta\varphi_{\text{out}} \pm (2m + 1)\pi$ ; (b)  $\Delta\varphi_{\text{in}} = \Delta\varphi_{\text{out}} \pm 2m\pi$ ,  $m = 0, 1, 2, \dots$

The numerical analysis in Fig. 4 is performed within the plane-wave approximation assuming vanishing residual absorption. The corresponding coupled wave equations can be found elsewhere [16]. The parameters chosen are  $R_{\omega} = 0.8$  and  $u_{10} = 1$  where the normalized input amplitude  $u_{10}$  is defined by  $u_{01} = \sigma a_{01} L$ , with  $\sigma$  - the nonlinear coupling coefficient and  $a_{01}$  - the input amplitude [21]. The physical meaning of the normalized input amplitude  $u_{10}$  can be understood from the expression for the stationary conversion efficiency  $\eta = \tanh^2(u_{01})$  in the case of single pass SHG of a plane wave with input amplitude  $a_{01}$  and perfect phase matching. The magnitude of the pulse shortening as well as the actual existence of such pulse compression capability, depend primarily on  $\Delta\varphi_{\text{in}}$ . The pulse shortening is maximized when  $\Delta\varphi_{\text{in}}$  is in the  $1.5\pi$ - $1.75\pi$  range and this range remains in the vicinity of  $1.5\pi$  when the phase mismatch  $\Delta kL$  is varied between 0.3 and 1.5 rad. For phase-mismatch exceeding 5 rad, the pulse shortening effect of the FDNLM becomes negligible.

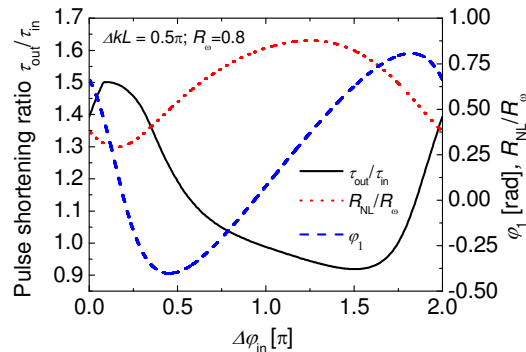


Fig. 4. Calculated pulse shortening ratio  $\tau_{\text{out}}/\tau_{\text{in}}$  (solid line), normalized nonlinear reflectivity  $R_{\text{NL}}/R_{\omega}$  (dotted line), and nonlinear phase shift  $\varphi_1$  of the fundamental wave (dashed line), as functions of  $\Delta\varphi_{\text{in}}$ .

The second mode-locking mechanism is based on self-phase modulation of the fundamental wave, due to cascaded  $\chi^{(2)}$  nonlinearity, where the cavity losses are modified by the cascaded  $\chi^{(2)}$  lens formation. This leads to fundamental wavefront defocusing/focusing with intensity dependent focal length. The resulting lens in combination with appropriate hard

or soft aperture causes strongly nonlinear intracavity loss modulation and eventually leads to mode-locking. In contrast to the third order Kerr effect, where the resulting lens effect is only positive (i.e. focusing lens), in cascaded second order nonlinearity the lens type depends on the sign of the phase-mismatch  $\Delta kL$  and it can be “+” which means a negative or diverging lens and “-“ which means a positive or converging lens. Also, the cascaded nonlinear phase shift can be saturated. The saturation intensity depends on the phase mismatch parameter  $\Delta kL$  and increases when moving away from the perfect phase matching point. In contrast to the FDNLM technique, the cascaded  $\chi^{(2)}$  lens mode-locking exists only for SHG at non-phase-matched condition, i.e. at  $\Delta kL \neq 0$ .

For better understanding of the cascading process and the way it leads to the phase shift, let us consider the case when a fundamental wave  $\omega$  is incident on a type-I nonlinear crystal with sufficiently large second order nonlinearity. In non-phase-matched condition the power is continuously converted from the fundamental to the second-harmonic (up-converted) and from second-harmonic to the fundamental (down-converted) at every half coherence length ( $L_c/2$ ). A part of the initial fundamental wave is up-converted into second harmonic according to  $2\omega = \omega + \omega$  and the two waves travel with different phase velocity. After typically one half coherence length, a part of the second harmonic is back-converted to the fundamental according to  $\omega_{bc} = 2\omega - \omega$  and this regenerated fundamental wave has different phase from the initial fundamental wave that has not been converted to second harmonic. The phase difference depends on the conversion efficiency and consequently on the intensity of the incident beam. If the radial distribution of the beam is not uniform, this will introduce curvature to the fundamental wavefront and the cascaded  $\chi^{(2)}$  process will act as a focusing or defocusing lens with intensity dependant focal length.

#### 4. Experimental results and discussion

Mode-locked operation is studied with four different output couplers, three DMs with partial reflectance (OC1 with 95%, OC2 with 80% and OC3 with 70%) at the fundamental wavelength and highly reflective for the second harmonic, and one DM, OC4, with partial reflectance (95%) at the fundamental and highly transmitting the second harmonic. The phase matching of the intracavity PPKTP crystal is controlled by changing the crystal operating temperature. The measured second-harmonic power versus temperature shows maximum conversion efficiency at 60.5°C (holder temperature) and ~12°C FWHM of the temperature phase-matching curve (Fig. 5). Stable passive mode-locking operation is observed, however, at higher temperatures, around 80°C. The optimum temperature varies in an interval of  $\pm 4^\circ\text{C}$  for each experiment.

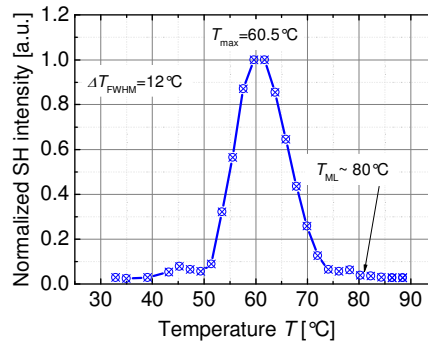


Fig. 5. Normalized single-pass second harmonic (SH) intensity as a function of the crystal holder temperature ( $T$ ) measured in the continuous-wave regime with OC4. Similar dependence is observed for all DMs.

A temperature induced phase-mismatch of  $\sim 6$  rad at 80°C is calculated using the temperature dependent Sellmeier equations for KTP [22]. Similar value of  $\sim 5.6$  rad is calculated using the value  $\theta = 0.27$  rad/°C for the phase-mismatch coefficient, obtained by

fitting the curve in Fig. 5 with theoretically calculated SHG signal for the resonator Gaussian beam as a function of the mismatch ( $\Delta kL/2$ ) =  $\theta\Delta T$  [23].

The highest output power and efficiency in mode-locked operation are achieved with the 30%-transmittance output coupler OC3. Figure 6 shows the dependence of the output versus the incident pump power. The laser threshold is 2.7 W. Passive mode-locking is observed in two distinct pump power ranges, from 10 to 10.5 W and from 14.7 to 16.2 W. In both regions, the output power is decreasing with the incident pump power. The modeling of the field distribution in the resonator shows two stability zones depending on the thermal lens in the Nd:YVO<sub>4</sub> AE. In the vicinity of the zone limits the mode size in the AE is changing. Therefore the efficiency is dropping due to non-optimum overlapping with the pump beam.

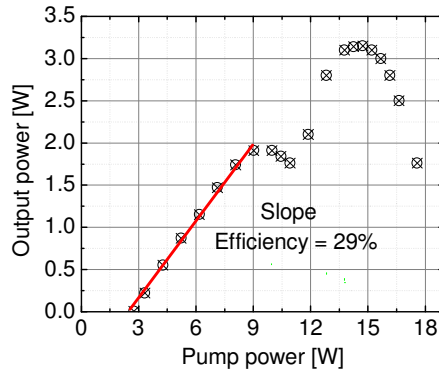


Fig. 6. Laser output power as a function of incident pump power using OC3.

The highest output power (3.1 W) in stable mode-locking regime is obtained at 15 W of incident pump power. In this case, the measured FWHM of the autocorrelation trace is 8 ps, Fig. 7(a), which corresponds to pulse duration of 5.2 ps, assuming  $\text{sech}^2$  pulse shape. The shortest pulse duration, 2.9 ps, see Fig. 7(b), is obtained using OC1 with 5% transmittance at the fundamental, highly reflecting at the second harmonic.

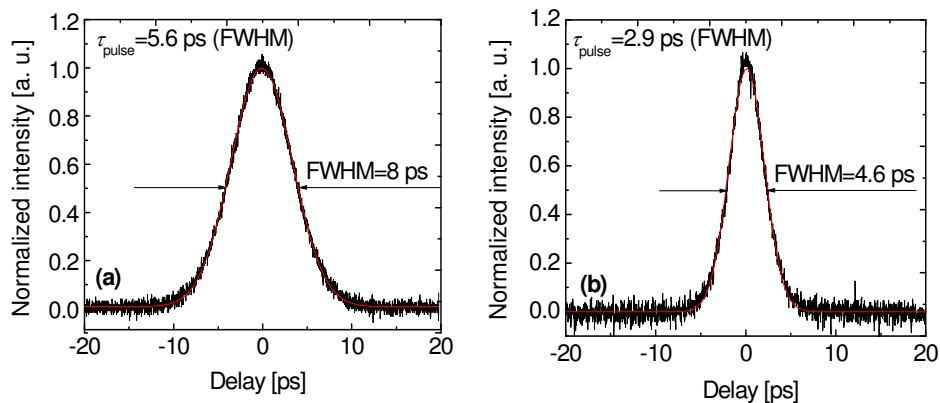


Fig. 7. Autocorrelation functions (black curves) and fits assuming  $\text{sech}^2$  pulse shape (red curves) using two dichroic output couplers with high reflectivity at the second harmonic, OC3 (a) and OC1 (b). The autocorrelation is measured by rotating-mirrors autocorrelator using non-collinear SHG.

Successful mode-locking is achieved with all the three dichroic OCs with different transmission at the fundamental wavelength and high reflection at the second harmonic. In

this case both nonlinear reflection and cascaded  $\chi^{(2)}$  lens process are simultaneously present. The nonlinear reflectivity of the FDNLM strongly depends on the phase-mismatch and reaches a maximum level when the second harmonic is perfectly phase-matched. On the other side, cascaded  $\chi^{(2)}$  lens exists only if there is a phase-mismatch. As can be seen from Fig. 8, this effect is, however, essential for obtaining short pulses, compare with Fig. 5. In fact, at the experimentally observed phase-mismatch, calculations predict negligible pulse-shortening effect from the FDNLM action as described in Fig. 4.

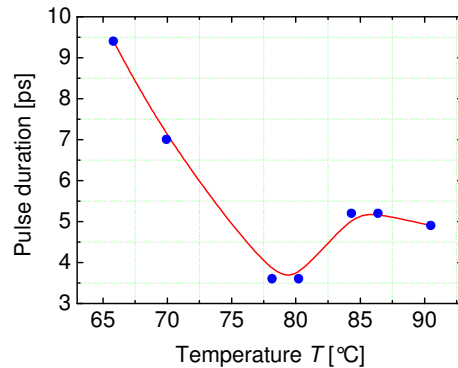


Fig. 8. Pulse duration (symbols) of the mode-locked Nd:YVO<sub>4</sub> laser at maximum output power with OC1 (see Table 1), measured in dependence on the NLC holder temperature  $T$ . The curve is just a guide to the eye.

In order to analyze the relative contribution of the two mechanisms to the mode-locking process we suppress the FDNLM effect by using OC4 having the same reflectivity as OC1 at the fundamental but high transmission at the second harmonic. The laser threshold is the same as in the case of using OC1. The stable output power in the mode-locking regime amounts to 0.7 W, at a pump power of 10 W. The measured autocorrelation trace width is 7.2 ps, corresponding to pulse duration of 4.7 ps assuming  $\text{sech}^2$  pulse shape. The mode-locking displays amplitude fluctuations less than 2% on millisecond time scale and long term stability with hours of continuous operation.

**Table 1. Summary of the laser performance with the four different dichroic output couplers.**

Output coupler $T$ [%] at 1064 nm & Reflectivity at 532 nm	OC1 5% & HR	OC2 20% & HR	OC3 30% & HR	OC4 5% & HT
Threshold pump power [W]	2.4	2.6	2.7	2.4
Slope efficiency [%]	6	27	29	9
Pump power range(s) with stable mode locking [W]	9 – 11 13.5	9 – 10.5 14.7 – 17.5	10 – 10.5 14.7 – 16.2	9 – 10.4 14
Output power [W]	<u>0.5 – 0.4</u> 1	1.9 – 1.8 <u>2.7 – 2.4</u>	1.9 – 1.8 <u>3.1 – 2.7</u>	<u>0.7 – 0.68</u> 1.1
Pulse duration ( $\text{sech}^2$ shape) [ps]	<u>2.9</u>	<u>4.5</u>	<u>5.2</u>	<u>4.7</u>

The results from the characterization of the laser performance with the four OCs are summarized in Table 1. With each output coupler, mode-locking is obtained in regions of negative slope in the input-output power dependence, as those shown in Fig. 6 for OC3. The two ranges of pump power in Table 1 correspond to the two rows of output power in the mode-locked regime. The underlined values for the output power correspond to the pulse durations given in the last row. At lower transmission of the output coupler at the fundamental (5% for OC1 and OC4) the self-sustained mode-locking is less stable in the higher power range. The optimum, for mode-locking, temperature of the crystal holder decreases by  $\sim 2^\circ\text{C}$ .



We attribute this behavior to the residual absorption in KTP and subsequent heating of the SHG crystal due to the increased average intracavity power. This effect requires more sophisticated temperature management system because KTP absorption mostly occurs at the second harmonic, the power of which strongly depends on the pulse length and thus changes dramatically when steady-state mode-locking is established or interrupted. Thus, the pulse duration values in Table 1 correspond to the output power range for which stable mode-locked operation is achieved.

## 5. Conclusion

We demonstrate operation of a passively mode-locked Nd:YVO<sub>4</sub> laser by intracavity frequency doubling in PPKTP. The cascaded  $\chi^{(2)}$  lens mode-locking process is the dominant mechanism for generation of pulse durations below 10 ps. Combination of the FDNLM technique with the cascaded  $\chi^{(2)}$  lens improves the long term stability and the self-starting capability of the system. The main result from the present study is the proof that stable mode-locking can be obtained up to the maximum output power achievable in the CW mode of operation. We achieve almost an order of magnitude higher average powers in comparison with [17] where cascaded  $\chi^{(2)}$  lens formation is realized with PPKTP in a Nd:GdVO<sub>4</sub> laser or with [19] where a combination with the FDNLM is realized with a KTP crystal in a Nd:YVO<sub>4</sub> laser. While a single operation point for mode-locking is found in [17], which lies in the region of thermal roll-over, it was possible in our set-up to adjust the mode-locking region to almost maximum pump level. The relatively low (350 mW) average output power achieved in [17] is also a consequence of the mismatch in the pump and laser mode sizes which had to be introduced in order to operate the laser close to its stability limits.

So far we are unable to reach the highest power level achieved with the FDNLM alone, but although 5.6 W were reported in [11] with the same laser material, the pulse durations in that work (20-ps) are roughly 4 times longer, see Table 1. We believe, however, that further power scaling of the present system will be possible by redesigning the laser cavity with special consideration of the thermal lens formation, shifting the region of stable mode-locking to yet higher output powers, the limit again being set by the TEM<sub>00</sub> power achievable in the CW regime.

As already mentioned, the technique described is feasible in wide spectral regions, and we plan to apply it in other types of lasers operating at wavelengths where no SESAMs exist, like Tm-lasers near 2  $\mu$ m. Moreover, this technique could be interesting also for Yb-lasers, which emerge as an alternative to Nd-lasers in the 1- $\mu$ m spectral range, with a huge potential for power scaling due to the smaller quantum defect, especially in combination with the thin disk concept. Although such systems, based on Yb:YAG, have already produced tens of Watts of output power at sub-picosecond pulse durations [5,24], one of the disadvantages of three-level Yb-based materials related to their longer lifetimes is that in the mode-locking regime they are more prone to Q-switching instabilities.

## Acknowledgments

This work has been supported by the Bulgarian Ministry of Science and Education under NSF grants VU-L-319/2007, Sofia University scientific research grant 294/2009, and DAAD (Germany) grant D/07/00333.